Molecular Vision 2021; 27:438-456 <http://www.molvis.org/molvis/v27/438>
Received 22 January 2020 | Accepted 6 July 2021 | Published 8 July 2021

Neuroprotective effect of minocycline on rat retinal ischemia-reperfusion injury

Xiaoli Li,[1,2] Zhiqiang Ye,[1] Shuaili Pei,[1] Dongliang Zheng,[1] Lin Zhu[1]

[1]Institute of Advanced Materials for Nano-Bio Applications, School of Ophthalmology and Optometry, Wenzhou Medical University, Wenzhou, China; [2]Henan Provincial People's Hospital and People's Hospital of Henan University, Henan Eye Institute, Henan Eye Hospital, Zhengzhou, China

Purpose: To examine the neuroprotective effect of minocycline on retinal ischemia-reperfusion (IR) injury in rats and investigate its possible mechanism of action.
Methods: Retinal IR injury was established by increasing the intraocular pressure in rats up to 110 mmHg for 60 min. The animals with retinal IR injury were intraperitoneally injected with 22.5 mg/kg minocycline twice a day for 14 days. The control group received the same amount of saline. Subsequently, funduscopic examination, retinal thickness measurement, retinal microvascular morphology, full-field electroretinography (ERG), retinal apoptotic cell count, and remaining retinal ganglion cell (RGC) count were performed. The expression of iNOS, Bax, Bcl2, IL-1α, IL-6, TNF-α, caspase-3, GFAP, Iba-1, Hif-1α, and Nrf2 was examined with real-time PCR and western blotting.
Results: Minocycline treatment prevented IR-induced rat retinal edema and retinal cells apoptosis at the early stage and alleviated retina atrophy, blood vessel tortuosity, functional photoreceptor damage, and RGC degeneration at the late stage of the IR injury. At the molecular level, minocycline affected retinal gene and protein expression induced by IR.
Conclusions: The results suggested that minocycline has a neuroprotective effect on rat retinal IR injury, possibly through anti-inflammation, antiapoptosis, antioxidation, and inhibition of microglial activation.

Retinal ischemia-reperfusion (IR) injury is associated with many ocular diseases and complications, including retinal vessel occlusion, diabetic retinopathy, and elevated intraocular pressure during vitreous surgery or after vitreo-retinal surgery. IR injury may cause a series of pathological problems, such as sterile immune response [1], vascular leakage [2,3], transcriptional reprogramming [4], and cell death [5,6]. Intraocular hypertension-induced retinal IR injury is a frequently used model for examining the pathogenesis, pathological change, and treatment of retinal diseases related to IR.

Minocycline (7-dimethylamino-6-dimethyl-6-deoxytetracycline) is a second-generation semisynthetic tetracycline analog with a broad spectrum of antibiotic activities. Recently, numerous studies have investigated the non-antibiotic properties of minocycline, including its anti-inflammatory [7], antiapoptotic [8], and antioxidative activities [9], as well as its neuroprotective effect [10,11]. Minocycline is a highly lipophilic molecule that can easily pass through the blood–brain barrier; thus, this molecule has been often used to treat central nervous system (CNS) diseases [12]. The retina has similar physiologic and biologic characteristics as the CNS. Therefore, minocycline may be a good drug candidate for the treatment of retina-related disease. Thus far, several preclinical and clinical studies have examined the neuroprotective effect of minocycline on ophthalmic diseases [13-16]. However, as only a few studies have investigated the effect of minocycline on retinal IR injury, the available results are controversial and inconclusive. For example, Abcouwer et al. [17] reported that minocycline prevents retinal inflammation (it inhibits inflammatory gene expression, leukocyte adhesion, and invasion) and vascular permeability following RI but does not affect neurodegeneration. In contrast, Chen et al. [18] suggested that the injection of 22 mg/kg minocycline may protect retinal function in IR injury. Thus, in this study, we further examined the neuroprotective effect of minocycline on retinal IR injury in rats and investigated the possible mechanism of action of minocycline.

Correspondence to: email: Lin Zhu, School of Ophthalmology & Optometry, Wenzhou Medical University, Institute of Advanced Materials for Nano-Bio, Applications, 270 Xueyuan Xi Road, Institute of Advanced Materials for Nano-Bio Applications, Wenzhou, Zhejiang 325000, China; Phone: 057788833806; FAX: 057788833806; email: akdz2554321@gmail.com

METHODS

The retinal ischemia-reperfusion injury model: Adult male Sprague-Dawley rats, weighing 250±10.0 g, were obtained from the Animal Center of Wenzhou Medical University. All animals were housed in an environment with a temperature of 22±1.0 °C, relative humidity of 50±1.0%, and a 12 h:12 h light-dark cycle. All animal studies (including the rat euthanasia procedure) were performed in compliance with

the regulations and guidelines of Wenzhou Medical University institutional animal care and conducted according to the American Association for Accreditation of Laboratory Animal Care (AAALAC) and Institutional Animal Care and Use Committee (IACUC) guidelines.

The ischemia-reperfusion injury model was established as follows: Animals were anesthetized with an intramuscular injection of 2% pentobarbital sodium (40 mg/kg bodyweight). Ischemia was induced in the right eyes by increasing the intraocular pressure (IOP). The anterior chamber was infused with sterile normal saline (NS) through a 30-gauge needle connected to a pressure transducer (Geuder®, D-69,126, Heidelberg, Germany) and an NS container via a three-way connector. The anterior chamber pressure was set to 110 mmHg by adjusting the height of the NS container. During the ischemia, the retina paled, and the fundus vasculature was narrowed, as observed with fundoscopy. Increased IOP was sustained for 60 min. Retinal edema was observed with optical coherence tomography (OCT) and indirect ophthalmoscopy.

The sham group was treated by inserting a 30-gauge needle into the anterior chamber through the corneoscleral junction, but not IR. Animals were handled in accordance with the Association for Research in Vision and Ophthalmology (ARVO) Statement for the Use of Animals in Ophthalmic and Visual Research.

Drug delivery and biomicroscopy observation: The experimental design involved two main groups of rats: the minocycline-treated group (Mino group) and the NT (Control) group that received no treatment. Specifically, the Mino group received intraperitoneal (IP) injections (twice daily for 14 days; initial dosage of 45 mg/kg 1 day before ischemia and then 22.5 mg/kg every 12 h), while the NT group received the same amount of normal saline. In addition, a sham group received normal saline and underwent sham surgery, as described above. All surgical animals were monitored with slit-lamp microscopy and fundoscopy to exclude ones that had complications caused by the operation, such as traumatic cataract, corneal opacity, and end ophthalmitis.

Morphology: Histology and optical coherence tomography: To investigate the effect of minocycline on the IR-induced morphological and retinal thickness changes, we performed OCT and image hematoxylin and eosin (H&E)-stained paraffin sections at 3 and 14 days after reperfusion. At a predetermined time (immediately and 3 and 14 days after reperfusion), six rats were anesthetized using 2% pentobarbital sodium (40 mg/kg bodyweight); both pupils were dilated using a single drop of 0.5% tropicamide and 0.5% phenylephrine eye drops (Santen Pharmaceutical Co., Ltd., Osaka, Japan). Rats were placed and fixed with an examiner to ensure that their eyeball was orthophoric, and the scan beam was perpendicular to the corneal surface. Spectralis HRA OCT (Heidelberg Engineering, Heidelberg, Germany) was used in the examination. Normal saline was administered to eyes every 2–3 min during the examination to keep the corneas lubricated. The retina was directly visualized during centering, and the optic nerve head was used as a landmark and located as the center while OCT images were taken (Software Version 6.3a). For each eye, one coronal image (right to left) and one vertical image (bottom to top) were collected crossing through the center of the optic nerve (ON), with four locations chosen at 0.5 mm intervals from the optic nerve for each image (i.e., the coronal image as shown in Figure 1), resulting in a total of eight locations for each eye. The resultant images were analyzed with ImageJ software to measure the retina's thickness at the locations described above. Corresponding neural retina thickness at the locations described above was measured by the distance from the ganglion cell layer's vitreal face to the apical face of the RPE as the whole retinal thickness.

For histology, six rats of each group were euthanized by intramuscular injection of 2% pentobarbital sodium (60 mg/kg body weight) at 3 and 14 days after reperfusion. Their eyes were enucleated and oriented by perpendicularly incising the wall toward the corneoscleral junction at the 3 o'clock location, and then fixed in an admixture of formalin, dehydrated alcohol, and glacial acetic acid (formalin, alcohol, and acetic acid [FFA] fixation fluid) for 24 h. The globes were embedded in paraffin and dissected vertically through the optic nerve head in 5 μm serial sections, which were stained with H&E. Histopathologic images were also analyzed with ImageJ software and measured for eight locations chosen at 0.5 mm intervals from the optic nerve for each image using the same method as the OCT images. The differences between them were the locations and the retinal layers. There were two more locations for the histology analysis than OCT in the perpendicular, all taken at 0.5 mm intervals. Because the histopathologic images were much clearer than OCT, the thickness of the different retinal layers was measured, including the retinal nerve fiber layer (RNFL), ganglion cell layer (GCL; RNFL + GCL), inner plexiform layer (IPL), and inner nuclear layer (INL).

Full-field ERG: After reperfusion for 1 and 2 weeks, six rats from each group were used for full-field electroretinography (ERG) examination with the International Society for Clinical Electrophysiology of Vision (ISCEV)-ERG program. We adopted the RETIport system with a custom-built Ganzfeld dome (Roland Consult, Wiesbaden, Germany), which was

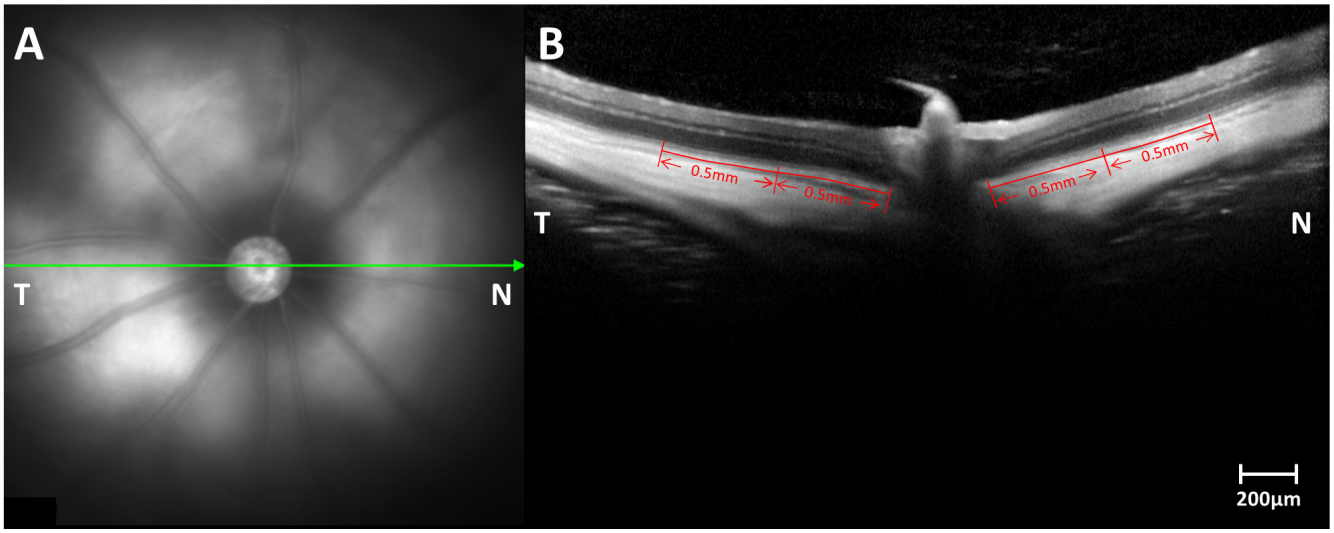

Figure 1. The locations of the retinal thickness were measured and analyzed using coronal OCT. **A**: The corresponding fundus photography micrographic pictures of optical coherence tomography (OCT). **B**: OCT coronal images and the locations of retinal thickness analyzed at 0.5 mm and 1.0 mm intervals from the optic nerve. Scale bar: 200 μm. N, nasal; T, temporal.

used to record standard full-field ERG. The pupils were dilated with a single drop of 0.5% tropicamide and 0.5% phenylephrine eye drop solution (Santen Pharmaceutical Co., Ltd., Osaka, Japan) and left to adapt in the dark for 2 h. Under dim red light, the animals were anesthetized as described above. A small amount of 2.5% methylcellulose gel was then applied to each eye, and a copper loop electrode designed specifically for rats was placed on the cornea to record the ERGs. Needle reference and ground electrodes were inserted into the cheek and tail, respectively. Dark-adapted ERG responses, including a rod response (dark adapt 0.01 ERG), standard combined ERG (dark adapt 3.0 ERG), and oscillatory potentials (OPs), were then recorded. The animals were allowed to adjust to the light for 5 min under a light intensity of 25 cd/m^2 and light-adapted responses, including a cone response (light adapt 3.0 ERG) and 30-Hz flicker. For each of the five stimuli programs, the average amplitudes and implicit times for each group were counted and analyzed.

TUNEL assay: Terminal deoxynucleotidyl transferase biotin-dUTP nick end labeling (TUNEL) assay was used to detect apoptotic cells. Twelve hours and 24 h after reperfusion were chosen as the time points for the TUNEL assay based on the preliminary data. Six animals were euthanized at each time point. The globes were quickly enucleated and oriented in the same way as for the frozen section. The globes were fixed in 4% paraformaldehyde (PFA) in 0.1 M PBS (1X; 120 mM NaCl, 20 mM KCl, 10 mM $NaPO_4$, 5 mM KPO_4, pH 7.4) buffer, for 24 h and dehydrated in 30% sucrose solution in 0.01 M PBS buffer for 4 h. The eyeball wall was sectioned serially at a thickness of 10–12 μm vertically crossing 6 and 12 o'clock through the optic nerve head using a cryostat. Six sections of each animal eye were chosen for TUNEL assay and the TUNEL Apoptosis Detection Kit (fluorescein isothiocyanate [FITC]; PH1456, Phygene Life Science, Fuzhou, China). The eyeball wall sections were digested with proteinase K at 37 °C for 30 min and then reacted with equilibration buffer at room temperature for 20 min. The tissue was reacted with a mixture of terminal deoxynucleotidyl transferase and FITC-dUTP buffer at 37 °C for 1 h. After several washings with PBS, the slides were stained with 4',6-diamidino-2-phenylindole (DAPI; PH0524, Phygene Life Science). Images were acquired with a confocal microscope (Zeiss LSM 710, Jena, Germany). The quantities of the apoptotic cells of the whole retinal layer of every section for each tissue were manually counted in a controlled blind manner and then were statistically analyzed.

Retrograde labeling and counting of the RGCs and retinal blood vessel staining: Because retinal IR can induce not only the loss of retinal ganglion cells (RGCs) but also impairment of retrograde axonal transport, retrograde labeling is an excellent way to evaluate the quantity of the remaining RGCs, which have the function of retrograde axonal transport after IR. In this study, the animals were anesthetized and prepared by shaving the skin 7 days after retinal refusion. According to the Rat Brain in Stereotaxic Coordinates [19], the operator incised the skin over the skull and located the superior bilateral colliculi, which were located 6.3 mm posterior to the bregma and 1.5 mm lateral to the midline on

both sides. After skull trepanation, 2 µl 10% 1,1'-dioctadecyl-3,3,3′,3′-tetramethylindocarbocyanine perchlorate (DiI, cat. no. 42,364, Sigma, St. Louis, MO) in dimethyl sulfoxide was slowly injected to a depth of 4.3 mm below the bony surface. The needle was left there for 5 min and then slowly withdrawn, after which the skin was sutured.

Seven days after the retrograde labeling operation, the rats were euthanized, and the globes were quickly enucleated and orientated. The anterior segment and vitreous were removed after fixation with 4% PFA and dehydration with a 30% sucrose solution. The retina was divided equally into four quadrants and incubated at 4 °C overnight in lectin from *Bandeiraea simplicifolia* BS-I isolectin B4 (IB4) FITC conjugate (1:100 dilution; cat. no. L2895, Sigma, St. Louis, MO) to visualize the retinal vasculature. After washing with PBS, the retinas were stained with DAPI. Finally, the retina was mounted flat on a slide for subsequent observation and imaging.

Using the same method as that for obtaining the histopathological sections to find the locations for imaging, we took images for each retinal quadrant at the positions from the ON at 0.5 mm intervals (i.e., from 0.5 mm, 1.0 mm, 1.5 mm, and 2.0 mm). Sixteen images were captured for each retina. The Z-stacks of images collected over all depths, on which all positive cells appeared with 200X magnification with the Zeiss LSM 710 confocal microscope, were projected as one composite image to include all labeled cells in the image. Two investigators counted the number of RGCs in each image in a blind manner, and the final data were averaged.

RNA extraction and real-time PCR: At 12 and 24 h after reperfusion, six rats from each group were euthanized, and their retinas were removed and stored at −80 °C for subsequent analyses. Total RNA was extracted from retinal tissues using TRIzol reagent (Invitrogen, Carlsbad, CA), dichloromethane (1,024,451,000, Sigma) and 2-propanol (I9516, Sigma), and then analyzed for purity with a NanoVue™ ultraviolet/visible spectrophotometer (28,956,057, GE Healthcare, St. Louis, MO). Consequently, 0.2 mg of total RNA from each sample was reverse transcribed with M-MLV reverse transcriptase into first-strand cDNA according to the manufacturer's instructions (Promega, Madison, WI). The primers were designed using Oligo 7.0 software; the sequences and product lengths are listed in Table 1. PCR reactions were performed in the Applied Biosystems 7500 Real-Time PCR System with 26SYBRH Green PCR Master Mix (PH1456, Phygene Life Science). The condition is 30 cycles of 94 °C for 20 s, 60 °C for 20 s, and 72 °C for 30 s. The results were normalized using the housekeeping gene *GAPDH* as a reference with the mRNA levels standardized in each group. For relative comparison, the cycle threshold (Ct) of the real-time PCR data was first converted to $2^{-\Delta Ct}$ before statistical analyses.

Western immunoblotting: The eyes of six rats were enucleated at 24 h after reperfusion. The retinas were peeled from the eyecup and immediately homogenized with 0.5 ml ice-cold lysis buffer. Insoluble material was removed with centrifugation at 120,000 xg at 4 °C for 20 min. According to the manufacturer's specifications, the final protein concentrations were determined using the bicinchoninic acid (BCA) protein assay kit (Pierce Biotechnology, Rockford, IL). GFAP (1:500 dilution in blocking solution), NRF2 (1:1,000) IL-6 (1:500), and IBA-1 antibodies (1:500), and HIF-1α (1:500) were used for immunodetection, and an anti-GAPDH polyclonal antibody was used to serve as a control to ensure that equivalent quantities of proteins were used for sodium dodecyl sulfate–polyacrylamide gel electrophoresis (SDS–PAGE). Protein bands were digitally analyzed with Quantity One 1-D Analysis Software (BioRad, Richmond, CA).

Table 1. Primers for genes in real-time PCR.

Gene	Sense primer	Antisense primer
iNOS	GCACAAAGTCACAGACATGGC	CCTGGGGTTTTCTCCACGTT
Bax	TGGCCTCCTTTCCTACTTCG	AAATGCCTTTCCCCGTTCCC
Bcl2	ACCCCTTCATCCAAGAATGCAA	TCTCCCGGTTATCATACCCT
IL-1α	CCAGAGCTGTTAATTGCCACA	AAAGACTCAGCACATGCCAT
IL-6	CAAACCTAGTGTGCTATGCCTA	TTTCAACATTCATATTGCCAGT
TNFα	GATCGGTCCCAACAAGGAGG	TTTGCTACGACGTGGGCTAC
Casp3	TCATGCACATCCTCACTCGT	AAACATGCCCCTACCCCACT
GFAP	GACCTGCGACCTTGAGTCCTTG	GAGCGAGTGCCTCCTGGTAACT
Iba-1	TGTCCTTGAAGCGAATGCTGGA	AACGTCTCCTCGGAGCCACT
hif1	ACTCTCAGCCACAGTGCAT	TCGGGCTCTTTCTTAAGCTTG
nrf2	CCAAGGAGCAATTCAACGAAG	TCGTCTTTTAAGTGGCCCAA

Statistical analysis: To compare the difference among groups at different time points, multivariate analysis of variance (MANOVA) tests were used to analyze the data of the retinal thickness measured with H&E staining, OCT, and ERG. One-way ANOVA tests were used to analyze the number of retinal apoptotic cells and the number of RGCs. For PCR, a two-sample Student *t* test was used. All data were displayed as the mean ± standard error of the mean (SEM). A p value of less than 0.05 was considered statistically significant.

RESULTS

Minocycline prevents morphologic changes in the rat retina, including the formation of blood vessels and retinal thickness after IR injury: The funduscopic examination (Figure 2) revealed hyperplasia, circuity, and dilation 24 h to 2 weeks after IR. However, reduced circuity and dilation were found in the Mino group compared to the NT group (Figure 2). This result was further confirmed with morphologies analysis of the small vessels (Figure 2D–F). Moreover, the NT group's fluorescence leakage suggested that the blood–retinal barrier was damaged after modeling (Figure 2E). In comparison, there were no fluorescence leakage and less vessel circuity and dilation in the Mino group (Figure 2D). These data suggested that minocycline prevents morphologic changes of the rat retina, including blood vessels induced by IR injury. There was no difference between the fellow eyes of two groups in the fundus photographs and the retinal vessel photographs, which suggested minocycline itself could not induce the retina abnormality.

Next, H&E staining and OCT were used to evaluate the morphology and changes in retinal thickness between groups (Figure 3 and Figure 4). The OCT photographs showed that retina edema and retinal detachment were seen immediately after IR (as the red arrow points out in Figure 4A,B) in the Mino group and the NT group. Compared to the sham surgery eye (Figure 3A), each retinal layer of the NT group at 3 days after IR was edematous (Figure 3C), while no retinal edema was observed in the Mino group (Figure 3B). At 14 days after IR, the retinas of the NT rats (Figure 3E and Figure 4F) were obviously thinner (especially the NFL, the GCL, and the INL) compared to those of the Mino group (Figure 3D and Figure 4F). These results suggested that minocycline may reduce rat retina edema at the early stage of IR and reduce retina atrophy (to some extent) at the late stage of IR injury.

Figure 5 shows the retinal thickness of different locations by measuring H&E staining and OCT photographs of the sham group, the NT group, and the Mino group at 3 days and 14 days after IR. The average retinal thickness measured with the H&E staining images was as follows: The sham group at 3 days was 97.4±2.00 μm, the Mino group at 3 days was 96.1±5.10 μm, the NT group at 3 days was 124.5±1.400 μm; the Mino group at 14 days was 97.4±2.10 μm, and the NT group at 14 days was 74.0±1.00 μm. The results of the respective corresponding group measured with OCT were 203.6±5.800 μm, 205.1±1.800 μm, 223.1±2.900 μm, 195.5±2.700 μm, and 170.3±1.200 μm. The average retinal thickness of the Mino group at 3 days after IR was much thinner than that of the NT group measured using H&E staining (96.1±5.10 μm versus 124.5±1.400 μm, $p<0.001$) and OCT photographs (205.1±1.800 μm versus 223.1±2.900 μm, $p<0.001$), which suggested minocycline reduced the rat retina edema caused by IR. Similarly, the average retinal thickness of the Mino group at 14 days after IR was much thicker than that of the NT group measured in H&E staining (97.4±2.10 μm versus 74.0±1.00 μm, $p<0.001$) and OCT photographs (195.5±2.700 μm versus 170.3±1.20 μm, $p<0.001$), which suggested minocycline reduced the retina atrophy caused by IR at 14 days. Figure 5 also shows statistical differences of the retinal thickness corresponding to the same position of different locations between the NT and Mino groups by measuring H&E staining and OCT photographs. The results show statistically significant differences in the retinal thickness corresponding to the same position between the two groups at 3 and 14 days.

Furthermore, we measured the thickness of different retinal layers, including the RNFL and GCL (RNFL + GCL), IPL, INL, and ONL at different locations with H&E staining (Figure 6). The most obvious difference was the RNFL + GCL and IPL between the NT group and the Mino group at 14 days after IR (23.1±0.40 μm versus 16.3±0.40 μm, $p<0.001$). The thicknesses of the RNFL+GCL by measuring the H&E staining photographs of the sham group, the Mino group at 3 days, and the NT group at 3 days were 23.8±0.50 μm, 21.9±0.20 μm, and 30.3±1.10 μm, respectively. The thicknesses of INL for the sham group, the Mino group at 3 days, the NT group at 3 days, the Mino group at 14 days, and the Mino group at 14 days were 18.8±0.60 μm, 20.0±0.50 μm, 16.5±0.50 μm, 16.4±0.40 μm, and 12.7±0.90 μm, respectively. These results suggest that IR causes edema at the early stage and atrophy at the late stage in the retina layer, especially the inner layer (RNFL+GCL). At the same time, minocycline could prevent these morphologic changes.

Minocycline partially prevents the rat retina functional damage caused by IR on ERG: We adopted standard full-field ERG to evaluate any functional damage to the rat retina. The evaluating indicators included the b-wave amplitudes of dark-adapted 0.01, the a-wave amplitudes, the b-wave amplitudes of dark-adapted 3.0, the OS_2 wave of the dark-adapted

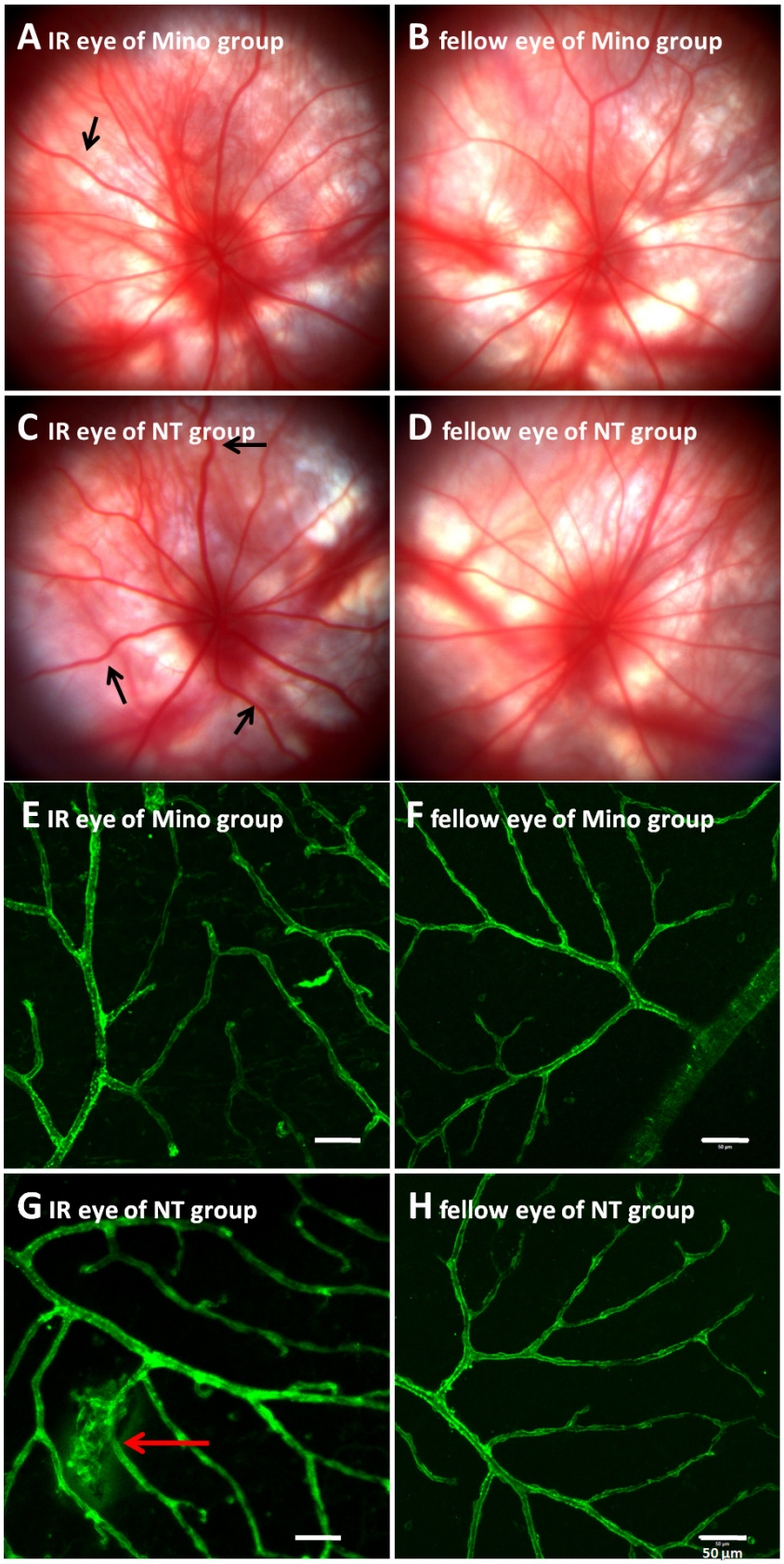

Figure 2. Fundus photography and retinal vessels (stained with IB4) in the Mino group and the no treatment (NT) group. The level of retinal vessel circuity and dilation was reduced in the minocycline treatment (Mino) group (**A, D**) compared to the NT group (**B, E**). The retinal vessels of the fellow eyes did not change after treatment (**C, F**). In **A** and **B**, black arrows point out the vessel's circuity and dilation. In **D**, **E**, and **F**, IB4 staining shows small blood vessel morphology. (In panel **E**, the red arrow points to the fluorescence leakage suggesting that the blood–retinal barrier was damaged).

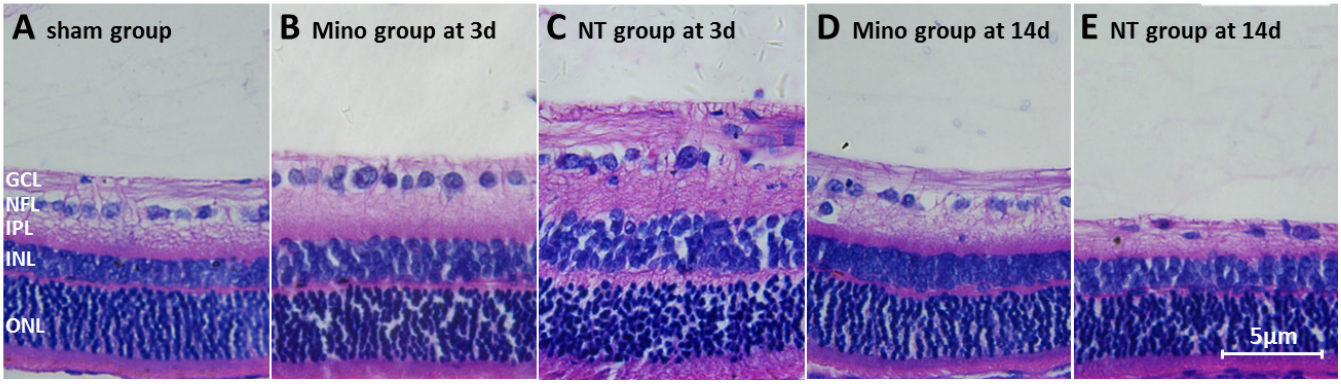

Figure 3. H&E staining for the retina of the non-minocycline treatment group and the minocycline treatment group at 3 days and 14 days after IR. (**A**) Sham group, (**B**, **D**) minocycline treatment (Mino) group, (**C**, **E**) no treatment (NT) group. At 3 days after ischemia-reperfusion (IR), edema is seen in the retinal layer of the NT group (**C**) but not in the Mino group (**B**). At 14 days after IR, the NT rats (**E**) have obviously thinner retinas compared to the Mino group (**D**), especially the nerve fiber layer, the ganglion cell layer, and the inner molecular layer. Scale bar: 5 μm.

3.0 oscillatory potential ERG, the a-wave amplitudes and the b-wave amplitudes of light-adapted 3.0, the N1-P1 wave times, and amplitudes of light flare 30 Hz ERG.

Table 2 shows all the ERG measurement parameters and the statistical results between the Mino group and the NT group. In general, all wave amplitudes in the NT group were lower than those in the sham group, and the appearances of some ERG patterns in the NT group were called "extinct," which means that all wave amplitudes were close to zero (Figure 7B). This appearance suggested that IR caused functional damage of the rat retina. In contrast, the wave amplitudes in the Mino group were higher than those in the NT group, and the two groups showed statistical differences, apart from the light flare 30 Hz ERG (Table 2), which

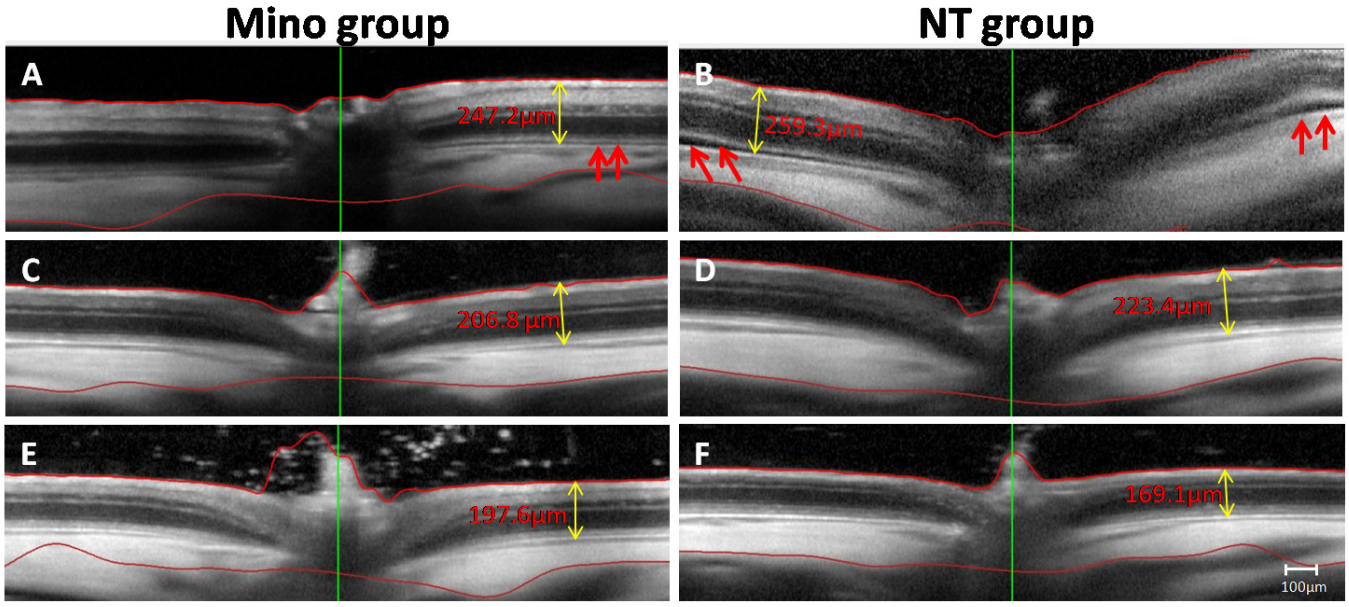

Figure 4. Representative optical coherence tomography (OCT) scans for the retinas of the minocycline group (**A, C, E**) and the non-minocycline treatment group (**B**, **D**, **F**) immediately after IR and at 3 days and 14 days after ischemia-reperfusion (IR). **A, B**: Retina edema and retinal detachment are observed immediately after IR as the red arrow points out in the minocycline treatment (Mino) group and the no treatment (NT) group. **C, D**: At 3 days after IR, the retina of the NT group was thicker than that of the Mino group. **E, F**: At 14 days after IR, the retina of the NT group was thinner than that of the Mino group. n = 6. Scale bar: 100 μm.

suggested that minocycline may partially prevent the functional retina damage caused by IR in rats.

The dark-adapted ERG programs were used to test the functions of the retinal rod cells. In this study, we adopted the dark-adapted 0.01 ERG and the dark-adapted 3.0 ERG to evaluate damage of the retinal rod cells after IR. The results showed that all wave amplitudes of the dark-adapted ERG in the Mino group were much higher at 1 week after IR than in the NT group, and some were even higher than in the sham group, which suggested that minocycline can prevent damage of the retinal rod cells and excite the retinal rod cells. However, the wave amplitudes of the dark-adapted ERG in the Mino group decreased at 2 weeks after IR compared to 1 week. Nonetheless, they were still higher than in the NT group with statistical significance. The results suggested that minocycline could not completely prevent or perhaps just delayed the damage of rod cells caused by IR.

The dark-adapted 3.0 oscillatory potential ERG is a relatively sensitive indicator that reflects the function of retinal microcirculation [20]. In this study, the OS_2 wave amplitudes had a statistically significant difference between the Mino group and the NT group at both time points, which suggested that minocycline prevents retinal microvascular damage caused by IR.

In the ERG program, the retinal cone cells system's functions were always tested by the light-adapted ERG programs, including the light-adapted 3.0 ERG and the light flare 30 Hz ERG. The results of light-adapted 3.0 ERG were similar to those of the dark-adapted 3.0 oscillatory potential ERG; the wave amplitudes in the Mino group were higher than those

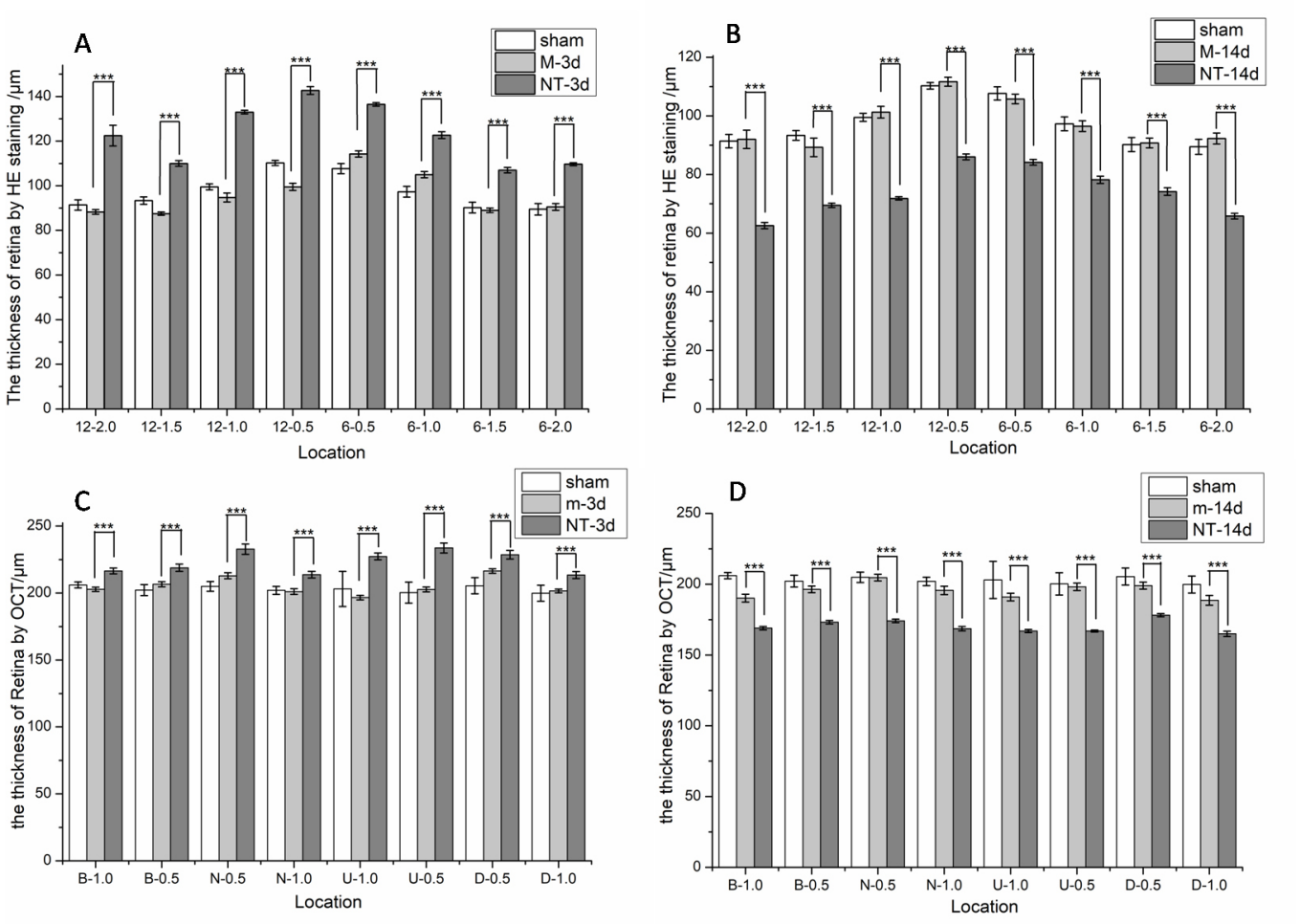

Figure 5. The retinal thicknesses of different locations by measuring H&E staining and OCT photography of the sham group, the non-minocycline treatment group, and the minocycline treatment group at 3 days and 14 days after IR. **A, B**: The retinal thickness with hematoxylin and eosin (H&E) staining. 12: 12 o'clock; 6: 6 o'clock. **C, D**: The retinal thickness with optical coherence tomography (OCT). B, bitemporal; N, nasal; U, up; D, down. n = 6. ***p<0.001.

in the NT group ($p<0.05$) and lower than those in the sham group, yet without statistical significance, which suggested minocycline may partially prevent retinal cone cell damage caused by IR. Furthermore, the b-wave amplitude in the light-adapted 3.0 ERG of the Mino group was lower than that in the sham group at 1 week and turned to normal at 2 weeks, which was different from the dark-adapted ERG programs. However, the wave amplitudes of P1-N1 in the Mino group for the light flare 30 Hz ERG at 1 week and 2 weeks were lower than in the sham group, but without statistical significance, thus suggesting that the IR damage to the retinal cone system is not obvious on the light flare ERG. Overall, minocycline

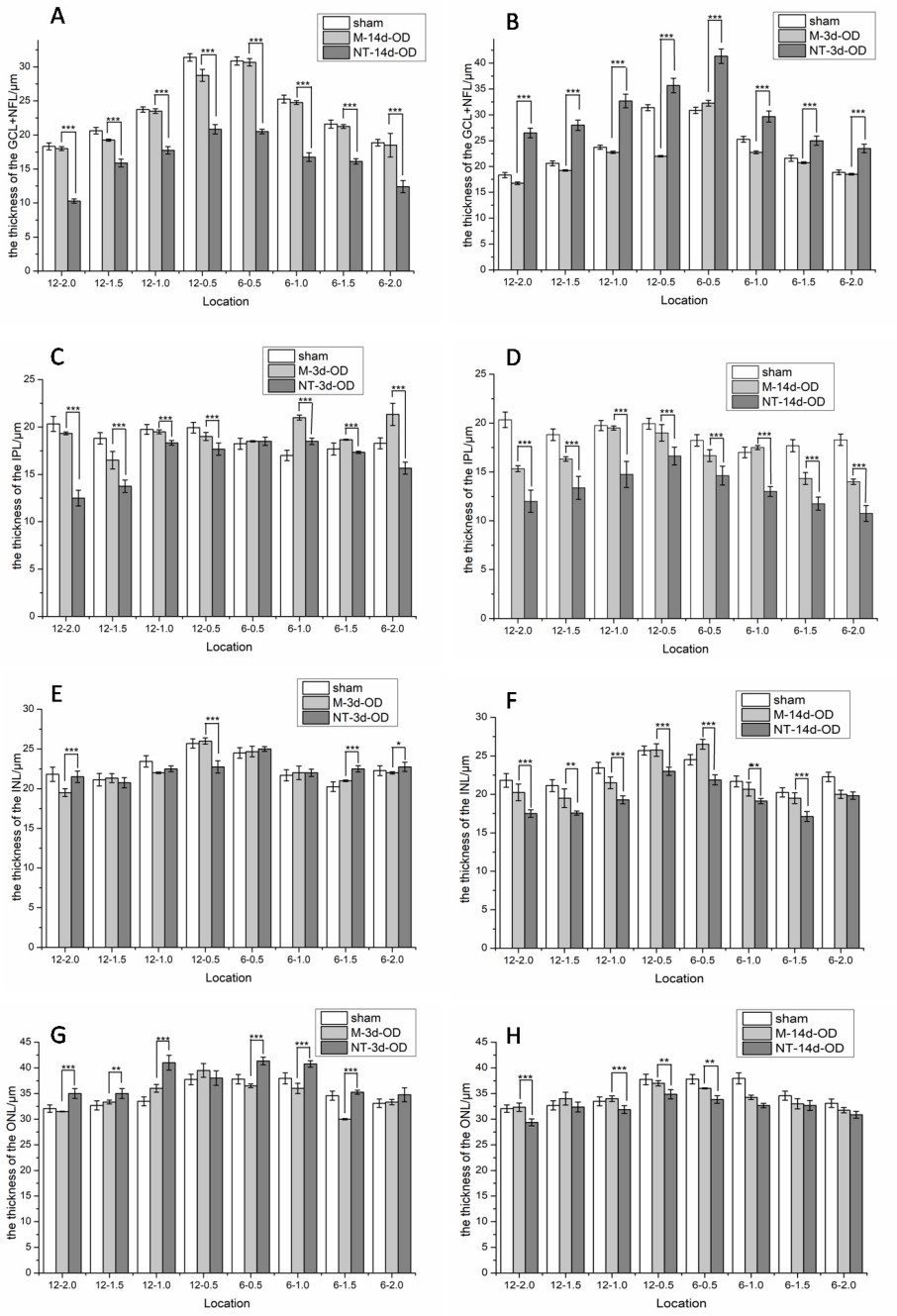

Figure 6. The thickness of each retinal layer at different locations measured using H&E staining at 3 days and 14 days after IR. **A**, **B**: Retinal nerve fiber layer (RNFL) and ganglion cell layer (GCL; RNFL + GCL). **C, D**: Inner plexiform layer (IPL). **E, F**: Inner nuclear layer (INL). **G, H**: Outer nuclear layer (ONL). n = 6, ***$p<0.001$.

Table 2. The results of ERG measurement.

ERG program	Time	Wave	Sham group	NT group	Mino group
Dark adapt 0.01 ERG	1w	b-wave(μV)	53.100±19.538	22.400±7.567**	56.120±14.080
	2w	b-wave(μV)	50.173±17.133	21.583±5.336*	46.100±15.447
Dark adapt 3.0 ERG	1w	a-wave(μV)	30.011±9.632	23.975±3.288*	37.260±9.306
		b-wave(μV)	62.107±13.430	12.750±2.439***	64.011±15.460
	2w	a-wave(μV)	31.270±8.379	14.850±2.250***	31.733±1.069
		b-wave(μV)	61.467±17.908	14.033±2.752*	35.057±17.087
Dark adapt 3.0 (Oscillatory Potentials, OPS)	1w	OS_2 (μV)	31.745±8.286	5.661±2.197**	29.693±13.620
	2w	OS_2 (μV)	29.448±9.118	5.918±3.846*	23.514±11.903
Light adapt 3.0 ERG	1w	a-wave(μV)	9.867±2.102	1.886±0.835***	8.102±1.063
		b-wave (μV)	11.854±3.650	2.350±0.797***	6.375±1.207
	2w	a-wave (μV)	9.263±2.750	1.880±0.689***	7.450±1.475
		b-wave (μV)	11.017±3.286	2.200±0.579**	10.078±4.152
Light flare 30Hz	1w	P1-N1(ms)	17.104±1.828	15.714±2.430	15.433±2.035
		P1-N1(μV)	3.451±1.720	2.396±0.828	2.355±0.718
	2w	P1-N1(ms)	17.214±1.822	15.929±1.880	16.857±2.734
		P1-N1(μV)	3.434±1.806	2.662±1.037	2.879±0.579

* Represents the significant difference between experiment group and control group. *** represents p<0.001; ** represents p<0.01; *represents p<0.05.

suspended the functional damage of the retinal cell system and microcirculation caused by IR.

Minocycline prevents retinal cell apoptosis caused by IR: In the preliminary experiment, six time points (3 h, 6 h, 12 h, 1 day, 3 days, and 7 days) after IR were selected for TUNEL assay measurements. We observed that retinal apoptotic cells appeared at 12 h and 24 h after IR. Consequently, 12 h and 24 h were further analyzed. As shown in Figure 8, the results showed fewer retinal apoptotic cells in the retina of the Mino group at 12 h (Figure 8A) and 24 h (Figure 8D) after IR compared to the NT group (12 h: Figure 8B and 24 h: Figure 8E). Apoptotic cells were mainly observed in the ganglion cell layer and the inner nuclear layer. Figure 8G shows the quantitative results (the average cell numbers of each visual field) of retinal apoptotic cells for each group. TUNEL-positive cells were counted in the retina 12 h and 24 h after IR. There was a statistically significant difference in the TUNEL-labeled cells between the Mino group and the NT group at 12 h after IR (7.97±1.06 cells/field versus 22.72±1.660 cells/field, p<0.001). At 24 h after IR, the difference between the Mino group and the NT group was decreased (12.33±2.380 cells/field versus 17.94±0.880 cells/field, p<0.01). To sum up, these results suggested that minocycline reduces retinal apoptosis caused by IR.

Minocycline protects RGCs against damage caused by IR: Evaluation of the survival of RGCs was performed with retrograde labeling. The RGCs labeled with DiI were counted at 14 days following retinal IR injury with or without minocycline treatment. Figure 9 shows pictures of retrograde-labeled RGCs in the retina; the red cells are the RGCs labeled with DiI, which had a good retrograde axonal transport activity. As shown in Figure 9, the number of labeled RGCs in the Mino group (Figure 9B,E) were higher than the NT group (Figure 9C,F).

To more accurately evaluate the surviving RGCs, the average cell number of retrograde labeled RGCs for each group was calculated (Figure 9G). There was a statistically significant difference in the number of RGCs between the Mino group and the NT group (179.81±19.090/field versus 128.00±16.720/field, p<0.01). These results suggested that minocycline protects RGCs against damage caused by IR.

Minocycline affects alterations of retinal gene expression after IR: The TUNEL assay results indicated that minocycline prevents retinal cell apoptosis caused by IR. Next, we hypothesized that minocycline might affect the retinal gene expression of inflammatory factors during the acute phase. We compared the gene expression levels of *iNOS*, *TNF-α*, *IL-1α*, *IL-6*, *Bcl-2*, *Bax*, *caspase-3*, *GFAP*, *Iba-1*, *Hif-1α,* and *Nrf2* in the Mino group and the NT group after IR (Figure

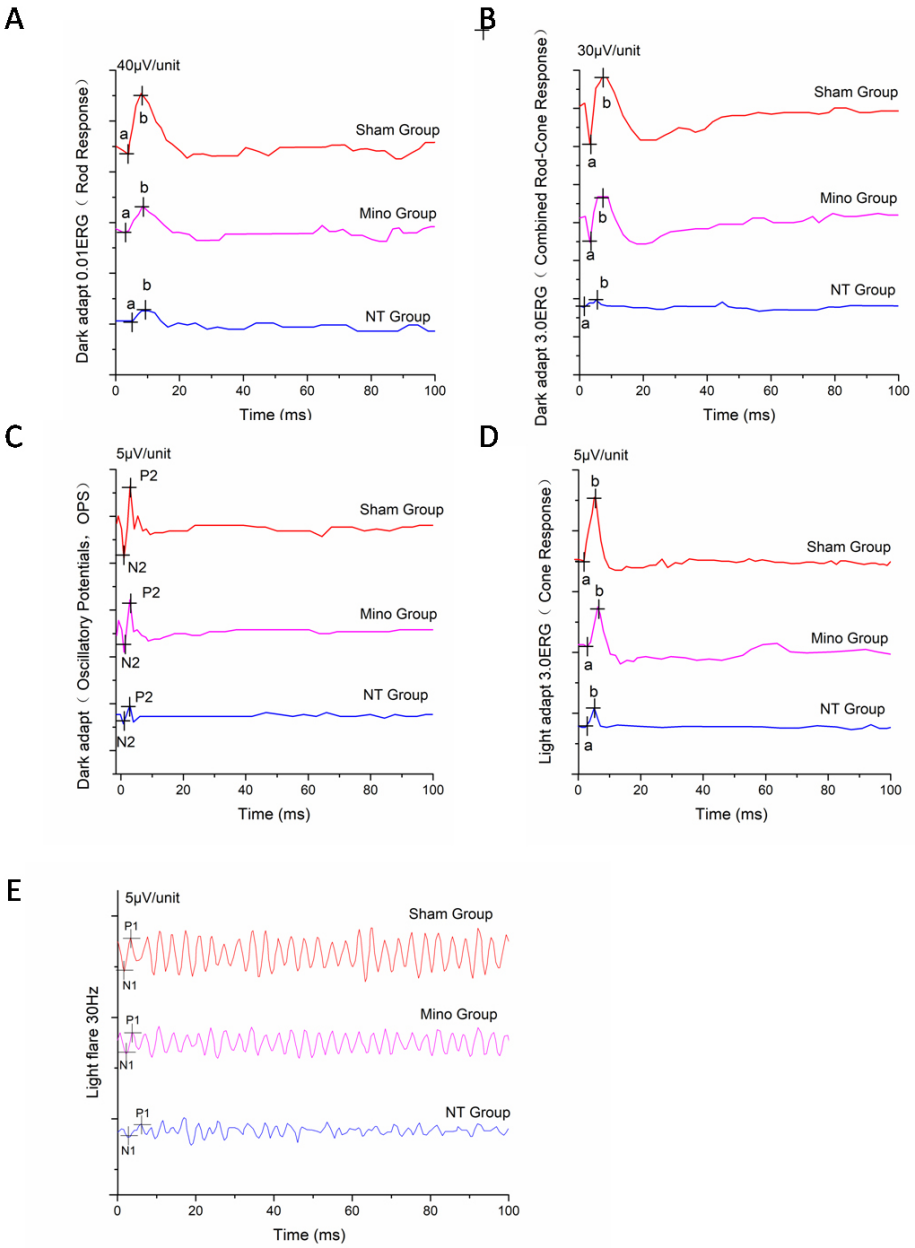

Figure 7. Representative electroretinogram images of each group at the 2 week point. **A**: The dark adapt 0.01 electroretinography (ERG) result image. **B**: Dark adapt 3.0 ERG result image. **C**: Oscillatory potentials result image. **D**: Light adapt 3.0 ERG result image. **E**: Light flare ERG result image.

10). In addition, we compared the protein expression level of GFAP, NRF2, IL-6, IBA-1, and HIF-1α in the Mino group and the NT group 24 h after IR (Figure 11). Because the fellow eye (the left eye) of each group did not receive IR injury, we assumed the retinal gene expression of the fellow eye was normal. We then quantified each group's value by obtaining the ratio of the experimental eye to the corresponding fellow eye.

As shown in Figure 10A, *iNOS* gene expression at 12 h and 24 h after IR of the NT group was 11.12±2.16-fold and 13.39±4.840-fold that of the corresponding fellow eyes (n = 5), while the corresponding expression of the Mino group was 0.81±0.46-fold and 3.28±1.38-fold (n = 5). The expression level in the Mino group decreased compared to that of the NT group, and the differences were statistically significant at 12 h and 24 h after IR ($p<0.001$ and $p<0.01$). iNOS is a type of enzyme that catalyzes nitric oxide (NO) from L-arginine. NO is an essential cellular signaling molecule, which helps modulate vascular tone. However, NO may be responsible for the degeneration of axons of retinal ganglion cells in the

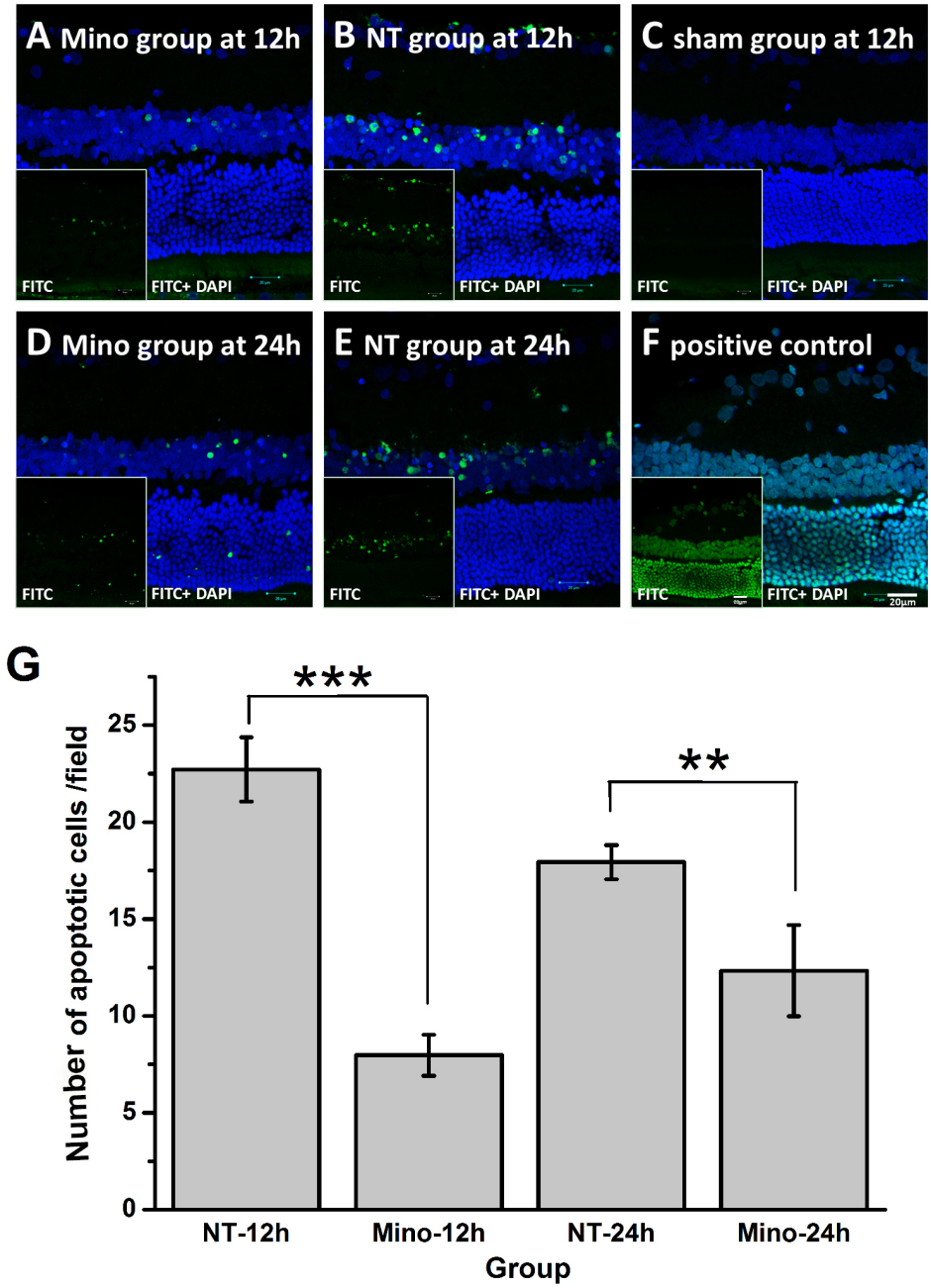

Figure 8. TUNEL assay results of the non-minocycline treatment group and the minocycline treatment group at 12 h and 24 h after IR. **A**–**C**: 12 h after ischemia-reperfusion (IR): (**A**) minocycline treatment (Mino) group, (**B**) no treatment (NT) group, and (**C**) sham group. **D**–**F**: 24 h after IR: **D**) Mino group, (**E**) NT group, and (**F**) positive control. We stained the cell nuclei with 4',6-diamidino-2-phenylindole (DAPI; blue) and Terminal deoxynucleotidyl transferase biotin-dUTP nick end labeling (TUNEL)-positive retinal cells with fluorescein isothiocyanate (FITC; green). The lower left part of each image indicates only the TUNEL-positive retinal cells. The number of TUNEL-positive retinal cells in the Mino group (**A** and **D**) at 12 h and 24 h was much lower than in the NT group (**B** and **E**). Scale bar: 20 µm. **G**: The average cell numbers of TUNEL-positive retinal cells for each visual field in each group (n = 6) at 12 h and 24 h after IR. NT-12 h: NT group at 12 h; Mino-12 h: Mino group at 12 h; NT-24 h: NT group at 24 h; Mino-24 h: Mino group at 24 h. ***p<0.001; **p<0.01.

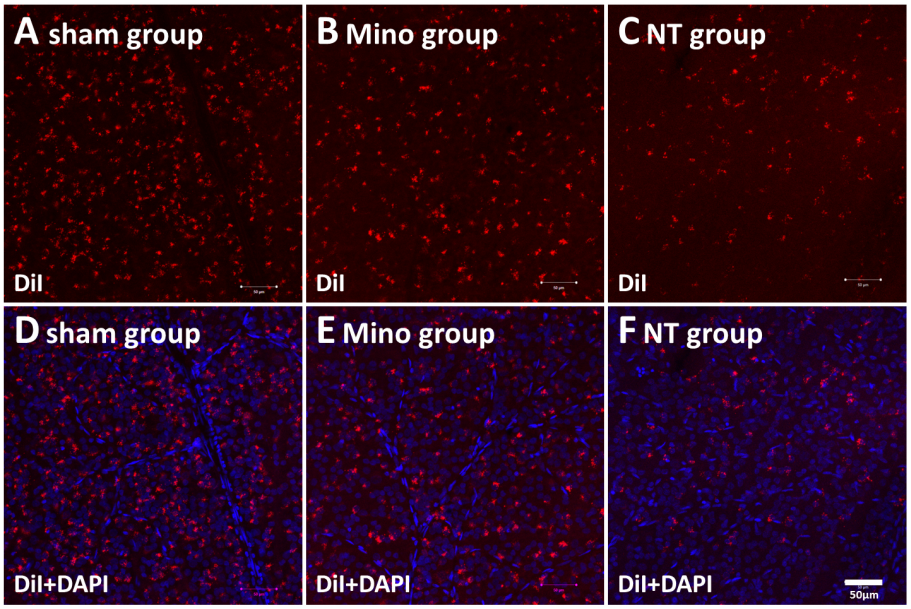

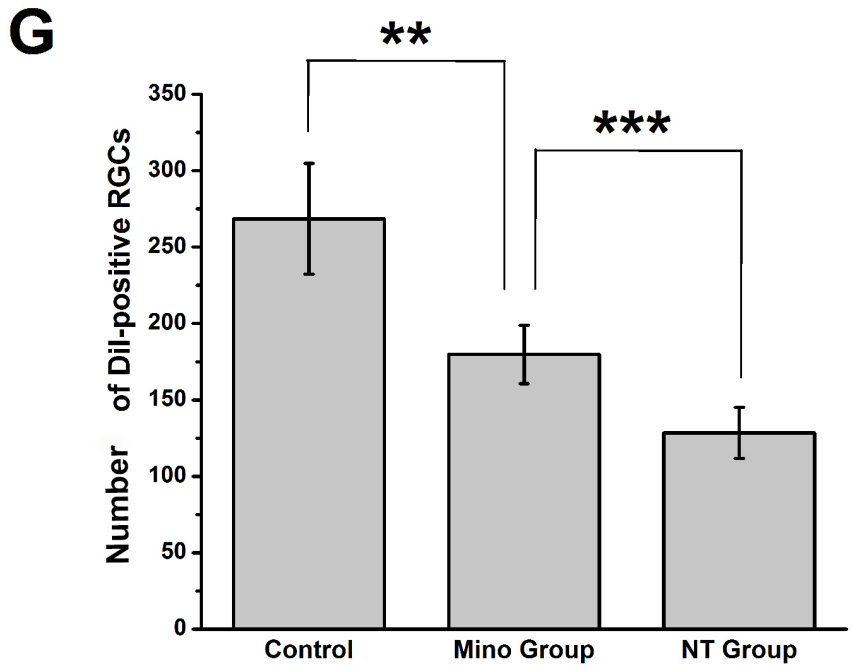

Figure 9. Retrograde-labeled RGCs in the retina at 14 days after IR injury. The picture of the retina was taken at bitemporal 1.5 μm from the optic nerve. **A, D**: Sham group; (**B, E**) minocycline treatment (Mino) group; (**C, F**) no treatment (NT) group. **A**–**C** show only cells with active retrograde transport were stained with 1,1'-dioctadecyl-3,3,3′,3′-tetramethylindocarbocyanine perchlorate (DiI; red). **D**–**F** show the merged images with cell nuclei stained with 4',6-diamidino-2-phenylindole (DAPI; blue). The number of retinal ganglion cells (RGCs) decreased markedly after IR injury compared with the sham group, while the minocycline prevented the numbers of RGCs from decreasing. Scale bar: 50 μm. **G**: The average cell numbers of retrograde-labeled RGCs for each visual field in each group (n = 6) at 14 days after IR. Sham: sham group without IR injury; NT-IR: NT group with IR injury; Mino-IR: Mino group with IR injury. ***p<0.001; **p<0.01.

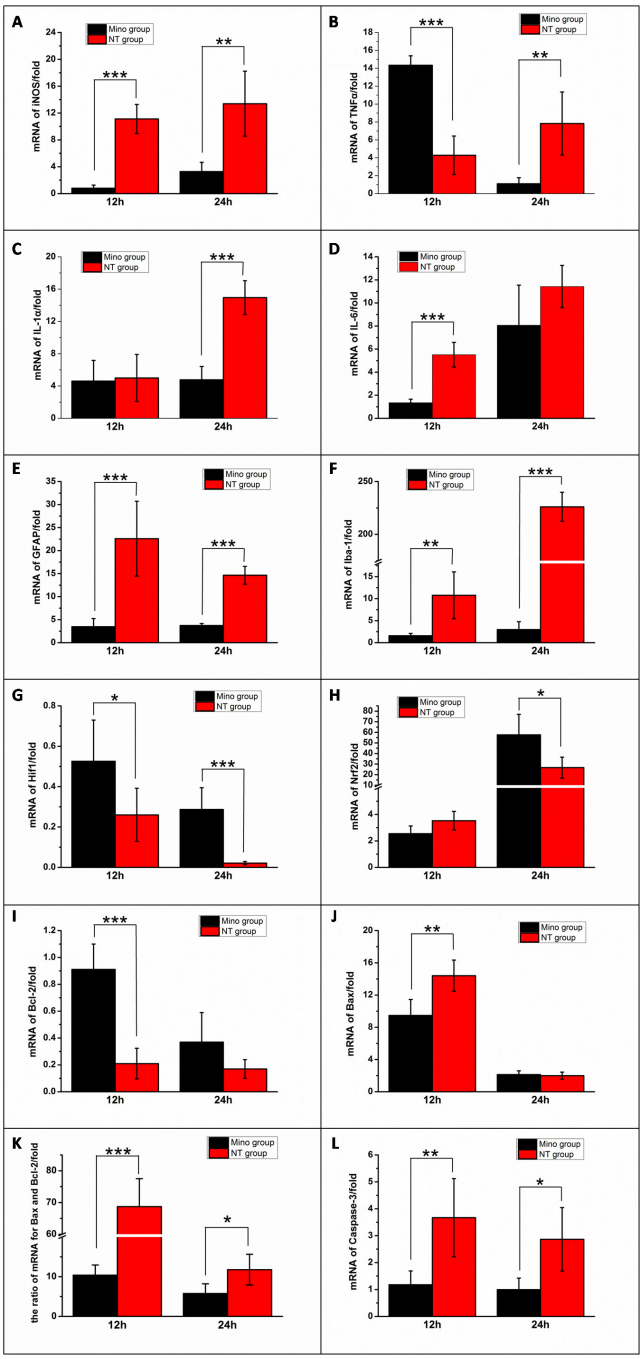

Figure 10. Gene expression of *iNOS*, *TNF-α*, *IL-1α*, *IL-6*, *Bcl-2*, *Bax*, *caspase-3*, *GFAP*, *Iba-1*, *Hif-1α*, and *Nrf2* in the neural retina evaluated with real-time PCR 12 h and 24 h after IR. The black box represents the minocycline treatment (Mino) group; the red box represents the no treatment (NT) group. The column value of each group was obtained from the ratio of the experimental eye to the fellow eye. Results from statistical analysis *p<0.05; **p<0.01; **p<0.001; n = 6.

glaucomatous optic nerve head [21]. Thus far, many studies have confirmed that NO is harmful to retinal cells in ischemia and reperfusion [22]. Thus, minocycline may protect RGCs in IR by regulating *iNOS* gene expression.

Several inflammatory genes increased statistically significantly at 12 h and 24 h after IR compared to the corresponding fellow eye. These genes included *TNF-α* (Figure 10B), *IL-1α* (Figure 10C), and *IL-6* (Figure 10D), and their ratios of the experimental eye to the fellow eye were much

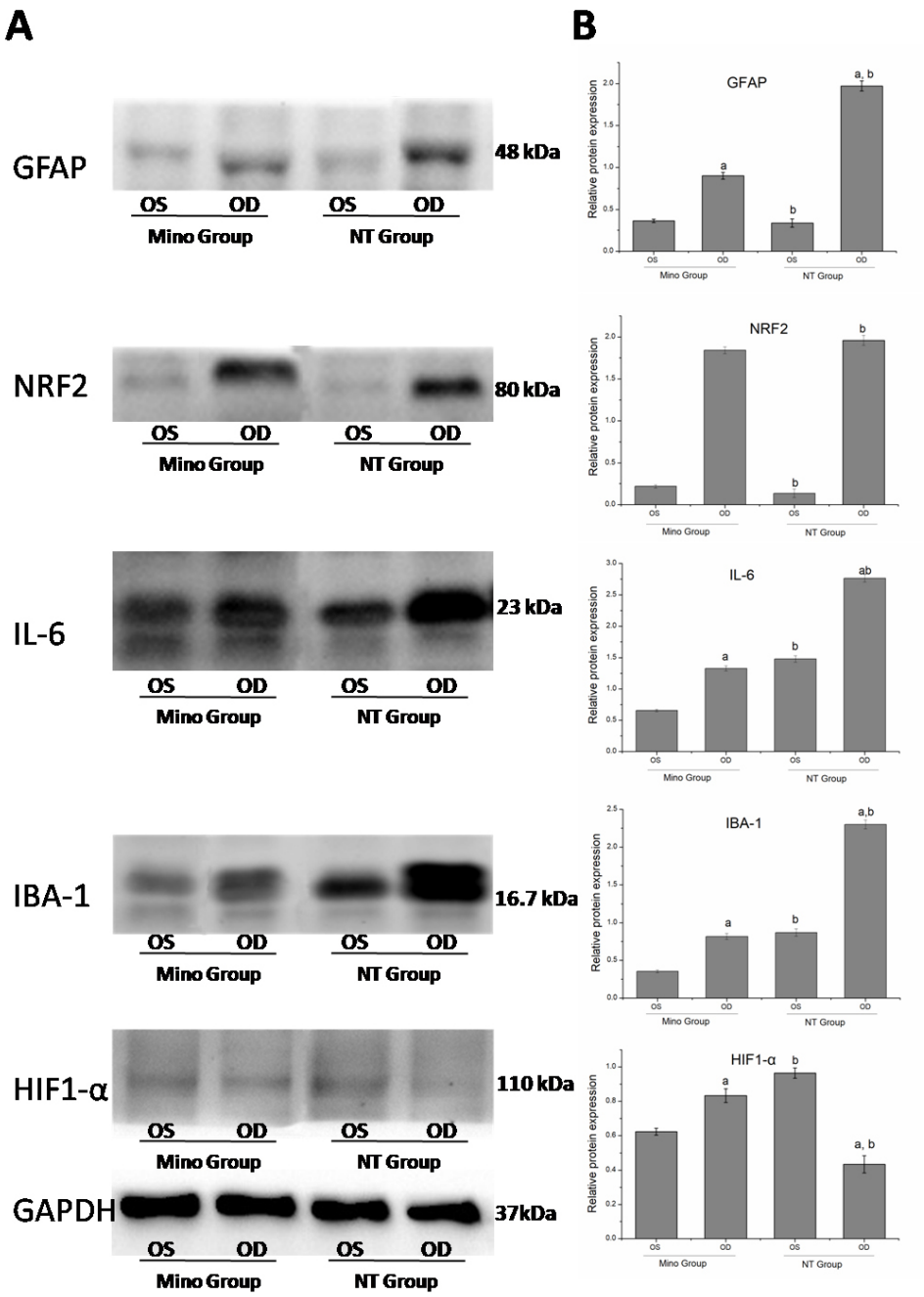

Figure 11. Western blotting (left) and quantification (right) of GFAP, NRF2, IL-6, IBA-1, and HIF-1α protein expression profiles in the neural retina 24 h after IR. [a]p<0.05 between the right eye of the no treatment (NT) group and the minocycline treatment (Mino) group; [b]p<0.05 between the left eye and the right eye of the minocycline (Mino) group. OS means left eye, and OD means right eye. n = 6.

larger than 1 at 12 h and 24 h after IR. However, compared to the NT group, the expression of *TNF-α* of the Mino group at 12 h and 24 h was much lower (p<0.05), which suggests that minocycline downregulates the expression of *TNF-α*. Moreover, the expression of *IL-1α* at 24 h and *IL-6* at 12 h between the Mino group and the NT group differed (p<0.05). The protein expression of IL-6 of the Mino group was lower than that of the NT group (p<0.05; Figure 11). These results suggested minocycline decreased the damage by downregulating the expression of inflammatory genes at the early stage after IR.

To test whether minocycline can inhibit the activation of glial cells, we detected the expression of *GFAP*, a marker of microglia cells, and *Iba-1*, a marker of a microglial cell. As shown in Figure 10E,F, minocycline can inhibit the activation of macroglia cells and microglia cells at 12 h and 24 h after IR. For *GFAP* gene expression, the inhibitory effect of minocycline was more statistically significant at 12 h after IR (Mino group versus NT group: 3.48±1.77 versus 22.59±8.140, p<0.001), whereas for *Iba-1*, the inhibitory effect of minocycline was much more statistically significant at 24 h after IR (Mino group versus NT group: 2.98±1.79 versus 226.06±13.73, p<0.001). The western blotting results further verified the changes from protein expression, as shown in Figure 11.

Hif-1α is overexpressed when cells trigger an adaptive response to hypoxia conditions. Interestingly, as shown in Figure 10G, the *Hif-1α* gene expression of the model eyes at 12 h and 24 h after IR was much lower than in the corresponding fellow eyes (12 h: 0.2601±0.1319-fold; 24 h: 0.021±0.008-fold). Minocycline statistically significantly abated the low expression of the *Hif-1α* gene at 12 h and 24 h after IR (12 h: 0.5259±0.2035-fold, p<0.05; 24 h: 0.2868±0.1078-fold, p<0.001). Moreover, the corresponding protein expression of *Hif-1α* in the Mino group at 24 h was lower than that in the NT group, as shown in Figure 11.

Nrf2 is a redox-sensitive transcription factor that binds to antioxidant response elements located in the promoter region of genes encoding many antioxidant enzymes and phase II detoxifying enzymes [23]. As shown in Figure 10H, *Nrf2* genes in the Mino group and the NT group were similarly highly expressed 12 h after IR (Mino group versus NT group: 2.55±0.5825-fold versus 3.53±0.71-fold). Twenty-four hours after IR, minocycline statistically significantly increased the expression of the *Nrf2* gene (Mino group versus NT group: 57.61±19.46-fold versus 26.65±9.91-fold, p<0.05).

According to the TUNEL assay results, IR can cause retinal cell apoptosis; therefore, we detected the expression of genes, including *Bcl-2* (Figure 10I), *Bax* (Figure 10J), and *caspase-3* (Figure 10L), associated with cell apoptosis. The *Bax* and *caspase-3* genes were overexpressed at 12 h (14.40±1.94-fold and 3.67±1.45-fold) and 24 h (1.99±0.44-fold and 2.86±1.18-fold) after IR in the NT group. *Bcl-2*, an antiapoptosis gene, remained at low levels after 12 h (0.21±0.11-fold) and 24 h (0.17±0.07-fold) after IR, which was consistent with the TUNEL assay. In the Mino group, *caspase-3* gene expression was lower than in the NT group at the corresponding time points (12 h: 1.18±0.51-fold, p<0.01; 24 h: 0.99±0.43-fold, p<0.05), which decreased statistically significantly compared with the NT group. The ratio of the *Bax* to *Bcl-2* expression is more meaningful for evaluating cell apoptosis; thus, the *Bax/Bcl-2* ratio was used to evaluate the expression of the two genes. Twelve hours after IR, the expression of *Bax/Bcl-2* (Figure 10K) in the Mino group was much higher than in the NT group (68.73±8.780-fold versus 10.39±2.570-fold, p<0.01).

DISCUSSION

This study systematically evaluated the neuroprotective effect of minocycline on retinal IR injury. The data suggest that minocycline may prevent retinal edema and retinal cells apoptosis induced by IR at the early stage and alleviate retina atrophy, blood vessel tortuosity, functional photoreceptor damage, and RGC degeneration during the late stage of IR injury in rats.

Morphologically, we found that IR injury may induce edema in retinal layers early after IR, especially in the ganglion cell layer and the nerve fiber layer, which is consistent with a previous report [23]. In contrast, minocycline treatment could reduce retinal edema. The overexpression of inflammatory factors, such as *IL-1α*, *IL-6*, and *TNF-α*, is the main reason for the occurrence of edema in the retina. The present results suggested that minocycline may reduce these inflammatory factors and protect the retina through its anti-inflammatory mechanisms during the acute inflammatory reaction stage. Previous studies also revealed the ability of active astrocytes to produce and secrete *TNF-α* in response to inflammatory stimuli. Kim et al. [5] discovered that *TNF-α* expression was a product of activated astrocytes and an initiator of necroptosis 12 h after retina IR. When IR injury occurs in the retina, *TNF-α* triggers the release of necroptosis factors that activate the caspase-independent signaling pathway, and in turn, induce necroptosis. In the present study, the genes related to apoptosis, such as *Bax* and *caspase-3* were overexpressed, while *Bcl-2* was downregulated. Moreover, cell apoptosis was observed in each retinal layer, including ganglion cells, bipolar cells, and photoreceptor cells, at an early stage after IR. Minocycline affected the expression of these genes and decreased apoptosis. In other retinal damage models, minocycline exerts its neuroprotective effects through antiapoptotic mechanisms [24]. Thus, it is believed that minocycline might be a promising antiapoptotic drug to treat retinal injury.

The fundus results indicated that IR induces retinal vessel circuity and dilation; this damage may be alleviated by minocycline. IB4 staining showed reduced small blood vessel hyperplasia, circuity, and dilation 2 weeks after IR. Dark-adapted 3.0 oscillatory potentials is a procedure of the ISCEV-ERG program that originated from the inhibitory

feedback loop activity of the inner plexiform layer, which can reflect the microcirculation of the retina. The data for the dark-adapted 3.0 oscillatory potentials in the present study showed that minocycline protects retinal microcirculation. Abcouwer et al. [17] reported that minocycline treatment might significantly inhibit IR-induced retinal vascular permeability and disrupt tight junction organization, which is consistent with the present results. Studies have also demonstrated that arteriole dysfunction, the major site for flow regulation, contributes to persistent retinal damage [25]. In addition, it is well-known that hypoxia-ischemia regulates many genes associated with inflammation, which may induce retinal vessel damage. Hein et al. [26] reported that endothelium-dependent NO-mediated dilation of retinal arterioles is impaired by ischemia-induced by elevated IOP. In the present experiment, minocycline inhibited the expression of *iNOS*, which may explain the low degree of vasodilation in the Mino group. Minocycline possibly prevents vessel dysfunction, including arterioles, via anti-inflammation, thus protecting retina nerve cells.

ERG is a crucial tool for evaluating retinal function. The ISCEV-ERG program includes five procedures described above that can comprehensively assess the photoreceptor function. The present study results showed that the b-wave amplitudes of the Mino group in dark-adapted 3.0 ERG were high (some were even higher than those in the sham group) 7 days after IR, which suggested the drug may excite retinal rod cells. Chen et al. ([18] reported that reduction in b-wave amplitudes caused by retinal ischemic injury was significantly counteracted by 22 mg/kg/day minocycline 7 days after IR. Moreover, Abcouwer et al. [17] reported that intravitreal injection of minocycline does not prevent ERG deficits following IR. The inconsistencies with the present study may be due to a difference in the elevated IOP and dosage of minocycline and the routes of drug delivery. In addition, intravitreal injection may lead to retina toxicity. Therefore, the effects of degrees of retinal injury by IR, the dosages of minocycline, and the methods of drug delivery on retinal function must be further investigated.

During the late stage after IR (14 days for rats), minocycline reduces retina atrophy, especially in the retinal ganglion cell layer, which is consistent with previous reports [18,27]. We also adopted retrograde labeling to evaluate the survival of RGCs after IR. The results showed that minocycline treatment increases the number of surviving RGCs, which have a good retrograde axonal transport activity after IR. Meanwhile, lower expression of GFAP, a marker of macroglia cells, and Iba-1, a microglial cell marker, was observed in the Mino group compared to the NT group. In many nervous system diseases, over-reactive microglia can distinguish between stressed and apoptotic cells, thus phagocyte viable neurons [28]. Minocycline can protect the retina by inhibiting microglial activation or in retinal diseases [15,24,29]. To sum up, the present results suggest that minocycline may inhibit activation of glial cells and protect RGCs against phagocytosis in retinal IR injury.

Typically, hypoxia induces *Hif-1α* overexpression. Jalal et al. [30] reported a significant increase in *Hif-1α* expression 1 week after unilateral carotid artery occlusion in rats. Moreover, Weidemann et al. [31] reported that retinal astrocytes are activated in an anoxic environment and secrete *Hif-1α* and *VEGF*, resulting in pathological neovascularization. In the present study, low expression of *Hif-1α* was found early after IR compared to the corresponding fellow eye. Why *Hif-1α* had such low expression at the early time point after IR is uncertain. However, we assumed that the time points were too short to reflect the whole expression, or the retinal cells were in a weaker hypoxia stage at 12 h to 24 h after IR. However, the expression of *Hif-1α* in the Mino group was higher than that in the NT group, which suggested minocycline affects the expression of *Hif-1α* .

Nrf2 is a vital stress response transcription factor. Previous studies showed that *Nrf2* has an important role in the pathogenesis of diabetic retinopathy [32], age-related macular degeneration [33,34], and other retinal diseases. In response to various stimulators, *Nrf2* translocases from the cytosol to the nucleus. This transcription factor binds to the antioxidant response element (ARE) located in the promoter region of a spectrum of oxidative stress-inducible genes [35]. *Nrf2* is an attractive therapeutic target for retinal diseases. In 2016, Nakagami et al. [36] found that the regulation of *Nrf2* may be a potential strategy for treating retinal diseases. In the present study, we found that *Nrf2* was upregulated in the rat retina 12 h and 24 h after IR; minocycline further augmented the upregulation. Tian et al. [36] reported that minocycline might exert protective effects against sevoflurane-induced cell injury via the *Nrf2*-modulated antioxidant response and inhibition of activation of the NF-κB signaling pathway. Furthermore, Kuang et al. [37] reported that minocycline delays retrovirus ts1-induced neurodegeneration through the upregulation of *Nrf2*. Thus, minocycline may promote upregulation of *Nrf2* to prevent retinal IR damage.

In conclusion, we further identified the neuroprotective effect of minocycline on rat retinal IR injury. Minocycline may become a promising drug candidate for treating diseases related to retinal IR injuries, such as glaucoma, retinal vessel occlusion, diabetic retinopathy, and ocular trauma. The minocycline mechanism of action underlying the neuroprotective

effect in retinal IR injury includes anti-inflammation and antiapoptosis, inhibition of activation of glial cells, and an antioxidative effect. However, this study did not examine the specific mechanism and pathway related to the antiapoptotic and antioxidative effect. Moreover, retinal IR injury of an animal model is different from human retinal diseases; therefore, whether minocycline can be used for human diseases must be further examined.

ACKNOWLEDGMENTS

The abstract of the article has been previously presented on 14 September 2018 of the 23rd Congress of the Chinese Ophthalmological Society in Hangzhou, China. The authors report no biomedical financial interests or potential conflicts of interest.

REFERENCES

1. Minhas G, Sharma J, Khan N. *Frontiers in immunology***7**, 444. Nakagami, Y. (2016). Oxid Med Cell Longev 2016; .
2. Zheng L, Gong B, Hatala DA, Kern TS. Retinal ischemia and reperfusion causes capillary degeneration: similarities to diabetes. Invest Ophthalmol Vis Sci 2007; 48:361-7. [PMID: 17197555].
3. Wilson CA, Berkowitz BA, Funatsu H, Metrikin DC, Harrison DW, Lam MK, Sonkin PL. Blood-retinal barrier breakdown following experimental retinal ischemia and reperfusion Exp Eye Res 1995; 61:547-57. [PMID: 8654497].
4. Ulbrich F, Lerach T, Biermann J, Kaufmann KB, Lagreze WA, Buerkle H, Loop T, Goebel U. Argon mediates protection by interleukin-8 suppression via a TLR2/TLR4/STAT3/NF-κB pathway in a model of apoptosis in neuroblastoma cells in vitro and following ischemia-reperfusion injury in rat retina in vivo J Neurochem 2016; 138:859-73. [PMID: 27167824].
5. Kim CR, Kim JH, Park HL, Park CK. Ischemia Reperfusion Injury Triggers TNFα Induced-Necroptosis in Rat Retina Curr Eye Res 2017; 42:771-9. [PMID: 27732109].
6. Wei T, Kang Q, Ma B, Gao S, Li X, Liu Y. Activation of autophagy and paraptosis in retinal ganglion cells after retinal ischemia and reperfusion injury in rats Exp Ther Med 2015; 9:476-82. [PMID: 25574219].
7. Kielian T, Esen N, Liu S, Phulwani NK, Syed MM, Phillips N, Nishina K, Cheung AL, Schwartzman JD, Ruhe JJ. Minocycline modulates neuroinflammation independently of its antimicrobial activity in staphylococcus aureus-induced brain abscess Am J Pathol 2007; 171:1199-214. [PMID: 17717149].
8. Pi R, Li W, Lee NT, Chan HH, Pu Y, Chan LN, Sucher NJ, Chang DC, Li M, Han Y. Minocycline prevents glutamate-induced apoptosis of cerebellar granule neurons by differential regulation of p38 and Akt pathways J Neurochem 2004; 91:1219-30. [PMID: 15569265].
9. Kraus RL, Pasieczny R, Lariosa-Willingham K, Turner MS, Jiang A, Trauger JW. Antioxidant properties of minocycline: neuroprotection in an oxidative stress assay and direct radical-scavenging activity J Neurochem 2005; 94:819-27. [PMID: 16033424].
10. Peng S, Wuu J, Mufson EJ, Fahnestock M. Increased proNGF levels in subjects with mild cognitive impairment and mild Alzheimer disease J Neuropathol Exp Neurol 2004; 63:641-9. [PMID: 15217092].
11. Zemke D, Majid A. The potential of minocycline for neuroprotection in human neurologic disease Clin Neuropharmacol 2004; 27:293-8. [PMID: 15613934].
12. Yong VW, Wells J, Giuliani F, Casha S, Power C, Metz LM. The promise of minocycline in neurology Lancet Neurol 2004; 3:744-51. [PMID: 15556807].
13. Krady JK, Basu A, Allen CM, Xu Y, LaNoue KF, Gardner TW, Levison SW. Minocycline reduces proinflammatory cytokine expression, microglial activation, and caspase-3 activation in a rodent model of diabetic retinopathy Diabetes 2005; 54:1559-65. [PMID: 15855346].
14. Kernt M, Thiele S, Hirneiss C, Neubauer AS, Lackerbauer CA, Ulbig MW, Kampik A. The role of light in the developement of RPE degeneration in AMD and potential cytoprotection of minocycline Klin Monatsbl Augenheilkd 2011; 228:892-9. [PMID: 21432767].
15. Sun C, Li XX, He XJ, Zhang Q, Tao Y. Neuroprotective effect of minocycline in a rat model of branch retinal vein occlusion Exp Eye Res 2013; 113:105-16. [PMID: 23748101].
16. Jiao X, Peng Y, Yang L. Minocycline protects retinal ganglion cells after optic nerve crush injury in mice by delaying autophagy and upregulating nuclear factor-κB2 Chin Med J (Engl) 2014; 127:1749-54. [PMID: 24791886].
17. Abcouwer SF, Lin CM, Shanmugam S, Muthusamy A, Barber AJ, Antonetti DA. Minocycline prevents retinal inflammation and vascular permeability following ischemia-reperfusion injury J Neuroinflammation 2013; 10:149-[PMID: 24325836].
18. Chen YI, Lee YJ, Wilkie DA, Lin CT. Evaluation of potential topical and systemic neuroprotective agents for ocular hypertension-induced retinal ischemia-reperfusion injury Vet Ophthalmol 2014; 17:432-42. [PMID: 24171811].
19. Paxinos G, Watson CR, Emson PC. AChE-stained horizontal sections of the rat brain in stereotaxic coordinates J Neurosci Methods 1980; 3:129-49. [PMID: 6110810].
20. Ferreri G, Buceti R, Ferreri FM, Roszkowska AM. Ophthalmologica. Journal international d'ophtalmologie. International journal of ophthalmology. Z Augenheilkd 2002; 216:22-6. .
21. Neufeld AH. Nitric oxide: a potential mediator of retinal ganglion cell damage in glaucoma Surv Ophthalmol 1999; 43:Suppl 1S129-35. [PMID: 10416755].
22. Lopez-Neblina F, Toledo AH, Toledo-Pereyra LH. Molecular biology of apoptosis in ischemia and reperfusion. J Invest Surg 2005; 18:335-50. .

23. Kim BJ, Braun TA, Wordinger RJ, Clark AF. Progressive morphological changes and impaired retinal function associated with temporal regulation of gene expression after retinal ischemia/reperfusion injury in mice Mol Neurodegener 2013; 8:21-[PMID: 23800383].

24. Peng B, Xiao J, Wang K, So KF, Tipoe GL, Lin B. Suppression of microglial activation is neuroprotective in a mouse model of human retinitis pigmentosa J Neurosci 2014; 34:8139-50. [PMID: 24920619].

25. Gidday JM, Zhu Y. Endothelium-dependent changes in retinal blood flow following ischemia Curr Eye Res 1998; 17:798-807. [PMID: 9723995].

26. Hein TW, Ren Y, Potts LB, Yuan Z, Kuo E, Rosa RH Jr, Kuo L. Acute retinal ischemia inhibits endothelium-dependent nitric oxide-mediated dilation of retinal arterioles via enhanced superoxide production Invest Ophthalmol Vis Sci 2012; 53:30-6. [PMID: 22110081].

27. Mathalone N, Lahat N, Rahat MA, Bahar-Shany K, Oron Y, Geyer O. Graefe's archive for clinical and experimental ophthalmology = Albrecht Von Graefes Arch Klin Exp Ophthalmol 2007; 245:725-32. .

28. Akhtar-Schafer I, Wang LP, Krohne TU, Xu HP, Langmann T. Modulation of three key innate immune pathways for the most common retinal degenerative diseases EMBO Mol Med 2018; •••:10-.

29. Scholz R, Sobotka M, Caramoy A, Stempfl T, Moehle C, Langmann T. Minocycline counter-regulates pro-inflammatory microglia responses in the retina and protects from degeneration J Neuroinflammation 2015; 12:209-[PMID: 26576678].

30. Jalal FY, Yang Y, Thompson JF, Roitbak T, Rosenberg GA. Hypoxia-induced neuroinflammatory white-matter injury reduced by minocycline in SHR/SP J Cereb Blood Flow Metab (Nihongoban) 2015; 35:1145-53. .

31. Weidemann A, Krohne TU, Aguilar E, Kurihara T, Takeda N, Dorrell MI, Simon MC, Haase VH, Friedlander M, Johnson RS. Astrocyte hypoxic response is essential for pathological but not developmental angiogenesis of the retina Glia 2010; 58:1177-85. [PMID: 20544853].

32. Zhong Q, Mishra M, Kowluru RA. Transcription factor Nrf2-mediated antioxidant defense system in the development of diabetic retinopathy Invest Ophthalmol Vis Sci 2013; 54:3941-8. [PMID: 23633659].

33. Lambros ML, Plafker SM. Oxidative Stress and the Nrf2 Anti-Oxidant Transcription Factor in Age-Related Macular Degeneration Adv Exp Med Biol 2016; 854:67-72. [PMID: 26427395].

34. Jarrett SG, Boulton ME. Consequences of oxidative stress in age-related macular degeneration. Mol Aspects Med 2012; 33:399-417. [PMID: 22510306].

35. Ishii T, Itoh K, Takahashi S, Sato H, Yanagawa T, Katoh Y, Bannai S, Yamamoto M. Transcription factor Nrf2 coordinately regulates a group of oxidative stress-inducible genes in macrophages J Biol Chem 2000; 275:16023-9. [PMID: 10821856].

36. Tian Y, Wu X, Guo S, Ma L, Huang W, Zhao X. Minocycline attenuates sevoflurane-induced cell injury via activation of Nrf2 Int J Mol Med 2017; 39:869-78. [PMID: 28260081].

37. Kuang X, Scofield VL, Yan M, Stoica G, Liu N, Wong PK. Attenuation of oxidative stress, inflammation and apoptosis by minocycline prevents retrovirus-induced neurodegeneration in mice Brain Res 2009; 1286:174-84. [PMID: 19523933].

Articles are provided courtesy of Emory University and the Zhongshan Ophthalmic Center, Sun Yat-sen University, P.R. China. The print version of this article was created on 8 July 2021. This reflects all typographical corrections and errata to the article through that date. Details of any changes may be found in the online version of the article.